

## Gyrotropic band gap optical sensors

Neluka K. Dissanayake,<sup>1</sup> Miguel Levy,<sup>1,a)</sup> Amir A. Jalali,<sup>1,b)</sup> and V. J. Fratello<sup>2</sup>

<sup>1</sup>Department of Physics, Michigan Technological University, Houghton, Michigan 49931, USA

<sup>2</sup>Integrated Photonics, Inc., Hillsborough, New Jersey 08844, USA

(Received 7 March 2010; accepted 16 April 2010; published online 6 May 2010)

Faraday-effect-active photonic band gap structures fabricated in iron garnet films are shown to provide a platform for optical sensing based on refractive index detection. Strong near-band gap-edge polarization rotations serve as a sensitive probe to cover-index changes in birefringent magneto-optic waveguides. A wide index range from air to  $n=1.6$  is explored. Device sensitivity is found to improve with cover index increase. Theoretical analysis of Bloch modes polarization state shows large near stop-band edge rotations and strong sensitivity to cover index. The combined effects of geometrical waveguide birefringence and Faraday rotation contribute to the strength of the sensor response. © 2010 American Institute of Physics. [doi:10.1063/1.3427404]

In the past several years there has been a growing interest in optical sensors based on refractive index (RI) detection.<sup>1–3</sup> A particular advantage of this type of detection is that the signal is related to sample concentration or surface density instead of total sample mass, a feature that is attractive for ultrasmall volume sensing.<sup>1</sup> Among the optical structures investigated for this purpose are photonic crystals.<sup>2,3</sup> Most of these rely on shifts induced on a resonant wavelength or on the spectral location of a band gap in response to RI changes. However, polarization changes in gyrotropic materials as a candidate for optical sensing have not been explored so far. Magnetophotonic-crystal-enhanced polarization effects provide an interesting alternative platform to explore the RI sensing capability of photonic crystals.<sup>4–9</sup> That is because gyrotropic photonic-band gap structures can be made to yield large polarization rotations sensitive to the nature of the cladding in waveguide configurations.<sup>6–9</sup> In this study we introduce a RI sensor based on the polarization rotation response to changes in cover index in magneto-optic waveguide photonic crystals. Figure 1 displays a schematic depiction of the device.

Previous work by some of us<sup>6–9</sup> has shown that there is a significant enhancement in polarization rotation near the band edges in magnetophotonic waveguide band gap structures for coupling forward traveling fundamental to back-scattered higher-order modes. Preliminary results suggest that this enhancement is due to the combined effect of Faraday rotation and birefringence in waveguide magnetophotonic crystals.<sup>6,8</sup> Although the origin of the effect is not fully understood, theoretical calculations of the orientation of the elliptical Bloch modes (semimajor axis) near the band edges show large rotations relative to the Bloch mode orientation outside the stop bands.<sup>7–9</sup> Here output Bloch mode orientation is taken with respect to the input TE polarization. There is some evidence that the experimentally observed near-band-edge magneto-optic rotations in these waveguide systems are not due to photon trapping,<sup>6–9</sup> a mechanism previously studied for Faraday rotation enhancement<sup>4,5</sup> making these phenomena particularly interesting.

The model used for the calculations in the present paper is based on a birefringent magneto-optic layered-stack structure with a bilayer unit cell (Fig. 2), presented in previous publications by some of the authors.<sup>7–9</sup> An alternating system of elliptically-birefringent local-normal-mode solutions to Maxwell's equations is introduced in adjacent layers. The Bloch states for the system are expressed as a linear combination of these local normal modes, subject to the Floquet–Bloch theorem. Forward- and backward-traveling local modes are allowed to differ in RI and elliptical-polarization state to account for the contra-directional coupling between modes of different order in the waveguide.<sup>7–9</sup> The Bloch mode in layer  $n$  is expressed as a linear combination of elliptically polarized partial waves of the form  $\hat{e}_{\pm}^{f,b} E_{0j} \exp[\pm i \omega n_{\pm}^{f,b} (z - z_n) / c]$ ,  $j=1-4$ , and  $i = \sqrt{-1}$ , for light of frequency  $\omega$  propagating in the  $z$ -direction.<sup>7–9</sup> Here superscripts  $f$  and  $b$  refer to the forward and backward propagating modes. The refractive indices  $n_{\pm}^{f,b}$  correspond to modes of opposite helicity,  $E_{0j}$ ,  $j=1-4$ , are partial-wave amplitude constants, and  $z_n$  is the location of the interface between layers  $n$  and  $n+1$ . The elliptical polarization-state unit-vectors  $\hat{e}_{\pm}^{f,b}$  are given by,

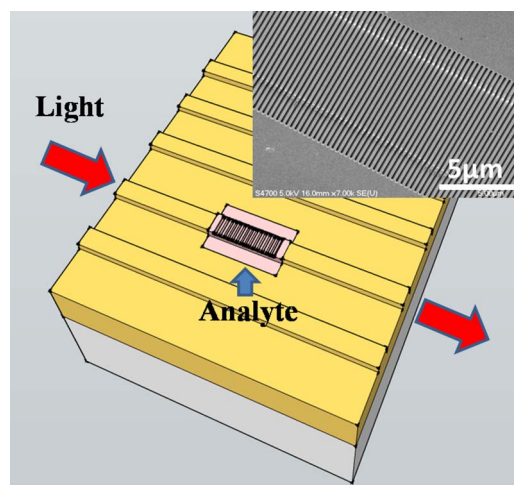


FIG. 1. (Color online) Schematic depiction of gyrotropic photonic band gap optical sensor. The analyte can be applied onto the photonic crystal as shown. The inset shows a scanning-electron micrograph of the Bragg grating region.

a)Electronic mail: mlevy@mtu.edu.

b)Present address: Electro-Optics Technology Inc., Traverse City, Michigan 49684, USA. Electronic mail: ajalali@eotech.com.

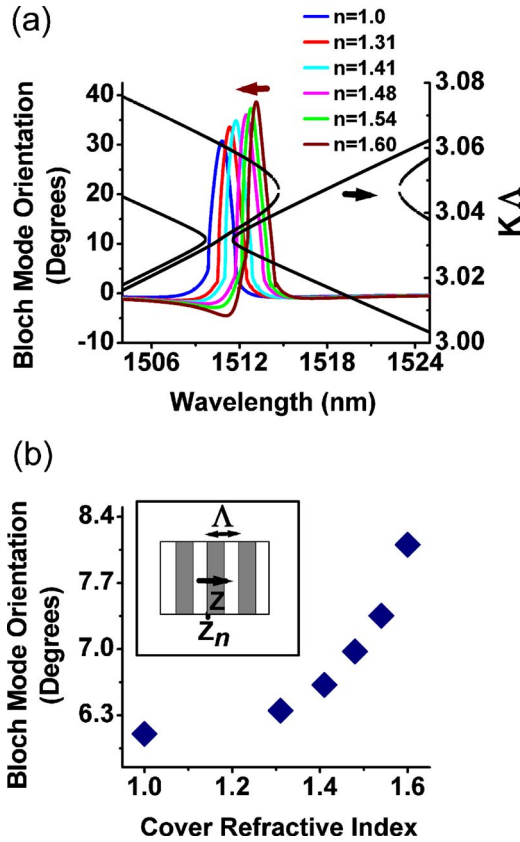


FIG. 2. (Color online) (a) Calculated band structure for a bilayer stack with  $\Lambda$  and the orientation of the semimajor axis of one of the Bloch modes for different cover indices. (b) Bloch mode polarization rotation for increasing cover index. Inset: layered-stack model.

$$\hat{e}_{\pm}^{f,b} = \frac{1}{\sqrt{2}} \begin{pmatrix} \cos \alpha^{f,b} \pm \sin \alpha^{f,b} \\ \pm i \cos \alpha^{f,b} - i \sin \alpha^{f,b} \\ 0 \end{pmatrix}, \quad (1)$$

with  $\tan 2\alpha^{f,b} = \Delta^{f,b}/g$ ,<sup>7-9</sup> where  $\Delta^{f,b} = (\epsilon_{xx}^{f,b} - \epsilon_{yy}^{f,b})/2$  are birefringence parameters.  $g$  is the gyrotropy parameter, related to the off-diagonal components of the dielectric tensor by  $\epsilon_{xy} = -\epsilon_{yx} = ig$  for magnetization along the propagation direction  $z$ . The other off-diagonal components  $\epsilon_{xz} = \epsilon_{yz} = \epsilon_{zx} = \epsilon_{zy} = 0$ . The model is optimized by switching off the gyrotropy parameter  $g$  and matching the center-wavelength and bandwidth of the model to experimentally determined transverse-electric (TE) and transverse magnetic (TM) stop bands. The gyrotropy is then turned back on and the stop bands and Bloch mode orientations are recalculated.

Figure 2(a) shows the calculated band structure and orientation of one of the Bloch modes as a function of cover index for fundamental to second-order-waveguide mode coupling. Here Bloch wave vector  $K = 2\pi/\Lambda$ , where  $\Lambda$  is the grating period. The model predicts not only a large enhancement in Bloch-mode polarization rotation (direction of semimajor axis) near the band edge but also a strong sensitivity of mode rotation to small RI changes in the waveguide cover index as shown in Fig. 2(b). Mode rotation is averaged over the main peak bandwidth of the mode. The orientation of all the Bloch modes shows a similar increasing trend with increasing cover index.

The waveguides used in this study are formed on single-layer bismuth-substituted rare earth iron garnet films grown

by liquid phase epitaxy on (100) gadolinium gallium garnet substrates. Standard photolithography and plasma etching are utilized to pattern 6  $\mu\text{m}$  wide 600 nm ridge-height waveguide structures on the film. One dimensional photonic band gap structures (Bragg gratings) are fabricated onto the ridge waveguide by ion beam milling in a Hitachi FB-2000A focused ion beam system.

Three sets of samples were investigated, all fabricated on 2.7  $\mu\text{m}$  thick  $\text{Bi}_{0.8}\text{Gd}_{0.2}\text{Lu}_{2.0}\text{Fe}_5\text{O}_{12}$  film. A 200  $\mu\text{m}$  long Bragg grating with period 337 nm and groove-depth 700 nm is denoted as sample 1. The film/substrate-interface to groove layer-thickness is 2.0  $\mu\text{m}$ . The ridge waveguide is 0.9 mm long. The waveguide mode refractive indices of the film before surface patterning measured on the film slab using prism coupler are 2.3041, 2.2616, and 2.1896 for the fundamental, first, and second order TE modes, respectively. Linear birefringence, defined as the difference between TE and TM mode indices measured for the first three modes are 0.0005, 0.0053, and 0.0130. The Faraday rotation per unit length in the film is 100°/mm.

Samples 2 and 3 consist of 200  $\mu\text{m}$  long photonic crystals with period of 348 nm and groove depths of 700 nm and 600 nm, with the film/substrate-interface to groove layer-thickness 2.0  $\mu\text{m}$  and 2.1  $\mu\text{m}$ , respectively. Their corresponding waveguide lengths are 0.8 and 1 mm. Prism coupler measurements of refractive indices for TE inputs for fundamental, first, and second modes are 2.3030, 2.2603, and 2.1882, respectively, while linear birefringence measured for the first three modes are 0.0008, 0.0051, and 0.0121, respectively. The specific Faraday rotation of this film is 80°/mm.

Optical transmission and polarization rotation tests are carried out for TE input light by end-fire fiber coupling from a tunable laser source with wavelength range 1480–1580 nm. The measurements are taken in a saturating magnetic field of 300 Oe applied collinear to the waveguide axis. Polarization rotation is defined here as the angle between the semimajor axis of the output polarization ellipse and the linear TE input polarization. The cover index of the waveguide photonic crystal was modified by applying commercially available RI liquids with refractive indices ranging from 1.31 to 1.60 onto the photonic crystal using a sharp-tip micromanipulator. Prior to applying the RI liquid, the polarization rotation response for air as cover index was also measured. After each successive RI measurement the samples were cleaned with a cleaning solvent and retested. The measurement for air as cover index was found to reproduce those prior to index liquid application.

Figure 3 shows the experimental polarization rotation measured for cover indices varying from  $n_c = 1.0$  to 1.6. These measurements are taken for the stop band formed by the coupling of forward-propagating fundamental and back-scattered second-order modes. The Bragg condition for the formation of multiple stop bands in waveguide photonic crystals is given by  $\lambda = (n_f + n_b)\Lambda$ ,<sup>6</sup> where  $\lambda$  is the free space wavelength,  $\Lambda$  the grating period, and  $n_f$  and  $n_b$  are average effective indices of the forward and backward propagating modes. It is found that the polarization rotation inside the stop band near the band edges increases significantly with increasing cover index. Figure 3(b) shows the measured rotation. The polarization rotation shown here is an average quantity, calculated by integrating the rotation over the entire bandwidth of the stop band and vicinity, using the polariza-

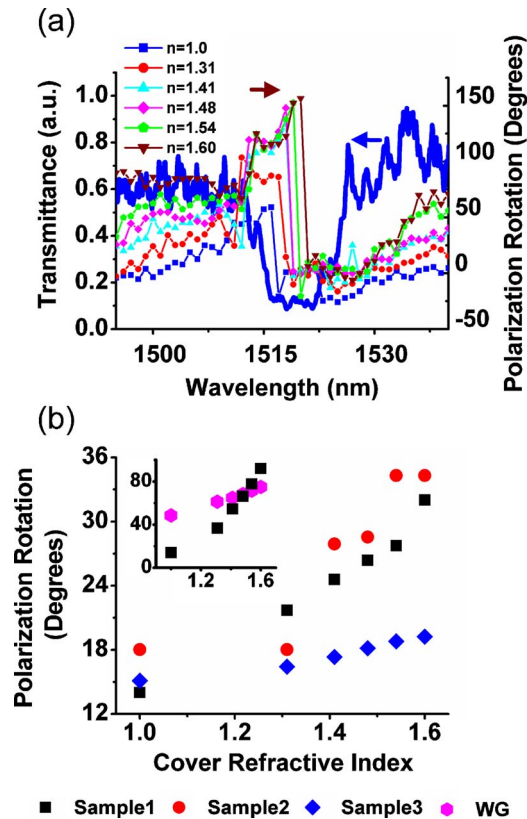


FIG. 3. (Color online) (a) Measured transmittance and polarization rotation for varying cover index of the waveguide photonic crystal for sample 1. (b) Polarization rotation measured for samples 1–3. The inset compares the polarization rotation vs cover index for a photonic crystal waveguide and for a plain waveguide (WG), showing a faster rate of change and stronger sensitivity in the photonic crystal structure. In order to be able to compare both types of rotations directly, the same baseline was used for both, namely, that of the input polarization, or zero rotation (TE mode).

tion outside the stop band as base line. A bandwidth average of the rotation is taken in order to reduce experimental measurement fluctuations and to fold in changes in the spectral shape of the response with cover index. The base line varies with cover index because of the rotation outside the grating structure. Defining a base line this way precludes folding in the rotation accrued in the waveguide before and after the photonic crystal structure. In this way the end result is purely due to the gyrotropic band gap effect. Differences in measured rotational strength are believed to result from grating groove-depth differences between the samples.

The polarization rotation of a plain waveguide (no Bragg grating) with the same cover indices was measured for comparison with that for a photonic crystal structure, resulting in a rotation of only half as much that inside the band gap of the photonic crystal at higher indices, and a lower rate of increase with cover index. It is evident that the gyrotropic band gap plays an important role providing higher sensitivity to the device. The combined effects of geometrical waveguide birefringence and Faraday rotation contribute to the strength of the sensor response. Generally, linear birefringence partially suppresses the Faraday rotation in a magneto-optic medium. However, the increase in cover index reduces the index contrast between cover and substrate leading to changes

in the polarization response. Moreover, spectral dispersion by the photonic crystal and its effect on Bloch mode polarization state lead to an enhanced sensitivity to cover index over a plain waveguide, as demonstrated experimentally in the present paper. Polarization changes in the photonic crystal over and above the plain waveguide baseline response are a strong function of cover index.

Both the theoretical calculation of Bloch mode orientation [Fig. 2(b)] and the experimental results [Fig. 3(b)] show that the slope of the polarization rotation versus cover index increases as the cover index on the photonic structure increases. The calculated rotation shown in Fig. 2(a) corresponds to only one Bloch mode. The experimental rotation shown in Fig. 3(a) is the resultant rotation generated by linear combination of all the propagating and evanescent Bloch modes of the system. The sensitivity of the device defined as the ratio between the rate of polarization rotation increase to cover index,  $S = \Delta\theta / \Delta n$  is estimated at  $71^\circ$  per RI unit in the higher (most sensitive) index range.

Among the attractive features of the gyrotropic band gap optical sensor are that it can be integrated onto a chip with other optical and electronic components, and its small sensing area ( $\sim 10^{-3}$  mm<sup>2</sup> in our case) requiring very small amounts of sample analyte ( $\sim 1$  pL) to activate the signal. In addition the sensor has a wide sensing range extending from air ( $n=1.0$ ) to  $n=1.6$ , making it suitable for variety of applications. The sensing range can be expanded up to  $n=1.9$ , with a sensitivity expected to be much higher at these higher cover indices. Device fabrication and operation are relatively simple, without stringent temperature stabilization requirements unlike resonant-cavity-based optical sensors.

In conclusion, we have investigated an optical sensor based on gyrotropic photonic band gap structures. Strong polarization rotation sensitivity near the stop band edges to cover index is demonstrated. Bloch mode polarization states are found to vary strongly with cover index and to track the changes in experimentally measured polarization rotations. The sensitivity inside the band gap is found to be much larger than in waveguides without Bragg gratings. The device demonstrates a sensitivity comparable to but no better than some other reported photonic-crystal sensors.<sup>1</sup> Theoretical calculations and experimental results show sensitivity improvement as the cover index of waveguide photonic crystal increases.

This material is based upon work supported by the National Science Foundation under Grant Nos. 0930525 and 0856650.

<sup>1</sup>X. Fan, I. M. White, S. I. Shopova, H. Zhu, J. D. Suter, and Y. Sun, *Anal. Chim. Acta* **620**, 8 (2008).

<sup>2</sup>N. Skivesen, A. Têtù, and M. Kristensen, *Opt. Express* **15**, 3169 (2007).

<sup>3</sup>T. G. Mackay and A. Lakhtakia, *IEEE Photonics Journal* **2**, 92 (2010).

<sup>4</sup>M. Inoue, K. Arai, T. Fujii, and M. Abe, *J. Appl. Phys.* **85**, 5768 (1999).

<sup>5</sup>S. Kahl and A. M. Grishin, *Appl. Phys. Lett.* **84**, 1438 (2004).

<sup>6</sup>M. Levy and R. Li, *Appl. Phys. Lett.* **89**, 121113 (2006).

<sup>7</sup>M. Levy, A. A. Jalali, Z. Zhou, and N. Dissanayake, *Opt. Express* **16**, 13421 (2008).

<sup>8</sup>A. A. Jalali and M. Levy, *J. Opt. Soc. Am. B* **25**, 119 (2008).

<sup>9</sup>M. Levy and A. A. Jalali, *J. Opt. Soc. Am. B* **24**, 1603 (2007).